Efficient peroxymonosulfate activation by microscale CuO coated melamine-cyanuric acid supramolecular toward tetracycline degradation

Ziru Shao, Shuangfei Zhang, Yonghong Shi, Deyong Wu*

Hubei Key Laboratory of Biologic Resources Protection and Utilization, School of Chemical and Environmental Engineering, Hubei Minzu University, Enshi, Hubei Province 445000, China

Table S1. Textural properties of as-prepared samples

Sample	S_{BET} (m^2 g^{-1})	V_{BET} (cm^3 g^{-1})	Pore size(nm)
CuO/MCSA-1	6. 18	0.023	15.59
MCSA	5.50	0.014	11.60

Table S2. The proportion of CuO in the CuO/MCSA-1measured by ICP-MS.

Sample	Measured Cu (wt%)	Calculate CuO (wt%)
CuO/MCSA-1	1.9822	2.9733

Table S3.Degradation efficiency and reaction rate constant of different materials

material	degradation efficiency (Contaminant, time)	reaction rate constant(min^{-1})
CuO/MCSA	84.1% (TC，30min)	0.0612
CuO/{010}$BiVO_4$[71]	97.1% (NOR, 60min)	0.0544
nAg/nZVI/AC[72]	90.1% (Toluene, 120min)	0.0866
MoO_3/g-C_3N_4[73]	81.13 % (TC,75 min)	0.0195
$ZnIn_2S_4$ /g-C_3N_4[74]	89.4% (Sulfamethoxazole,120 min)	0.0587
g-C_3N_4/$NiFe_2O_4$ /Ag[75]	92.1% (TC, 120 min)	0.0450

* Corresponding author.
E-mail address: wdy001815@126.com (D. Wu)

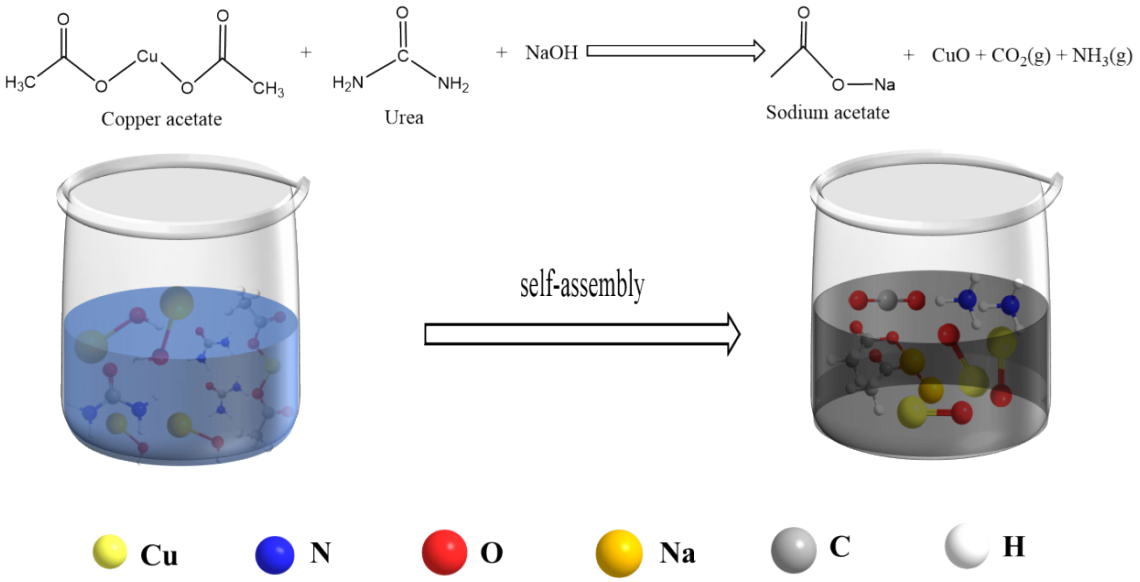

Fig.S1. Schematic procedure of CuO nanoparticles.

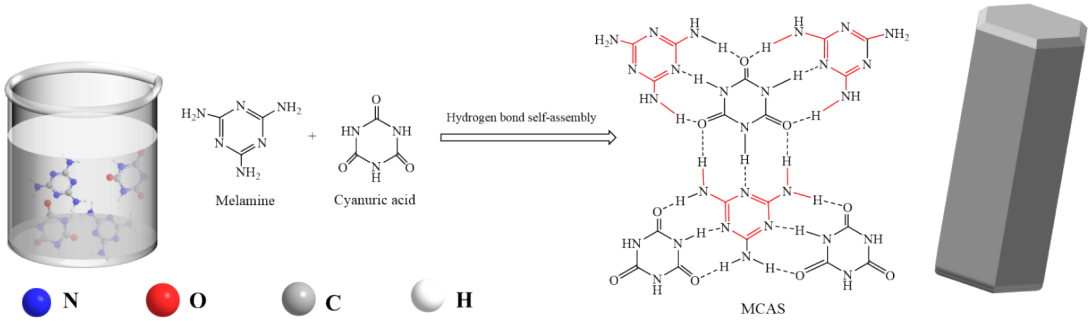

Fig.S2. Schematic procedure of MCSA.

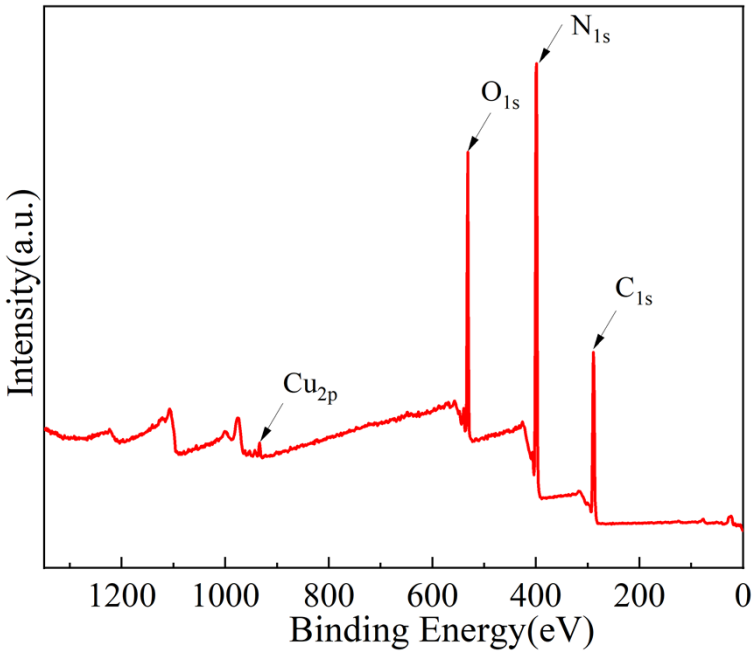

Fig.S3 The survey XPS spectrum of CuO/MCSA-1

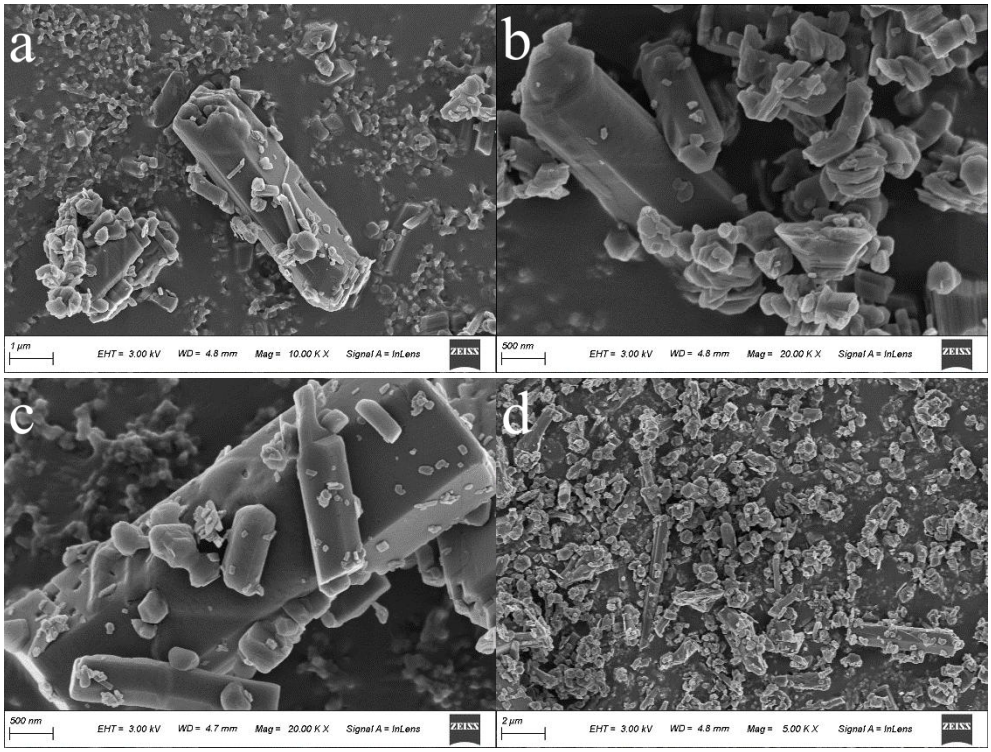

Fig.S4 SEM images of CuO/MCSA-2 (a) CuO/MCSA-3 (b) CuO/MCSA-4 (c) and CuO/MCSA-5 (d).

Fig.S5.TGA diagrams of CuO/MCSA-1.

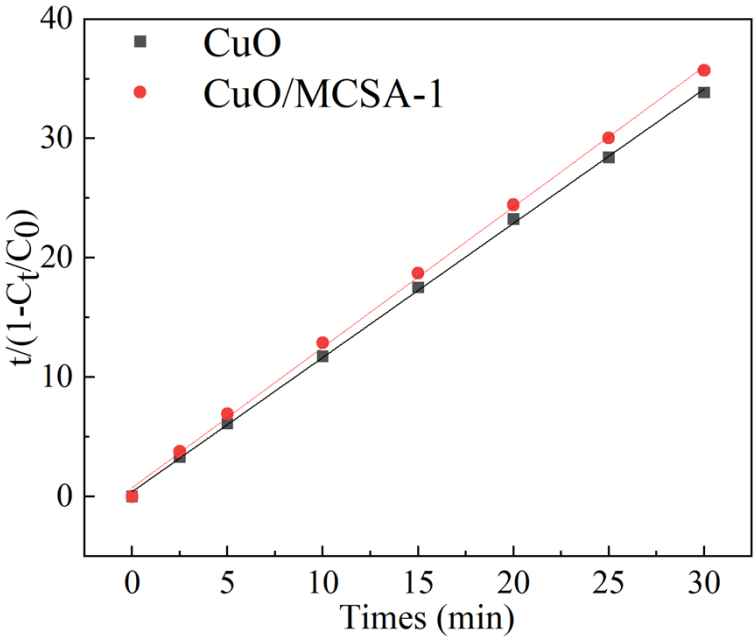

Fig.S6 The kinetic models of TC degradation by CuO/PMS system and CuO/MCSA-1/PMS system.

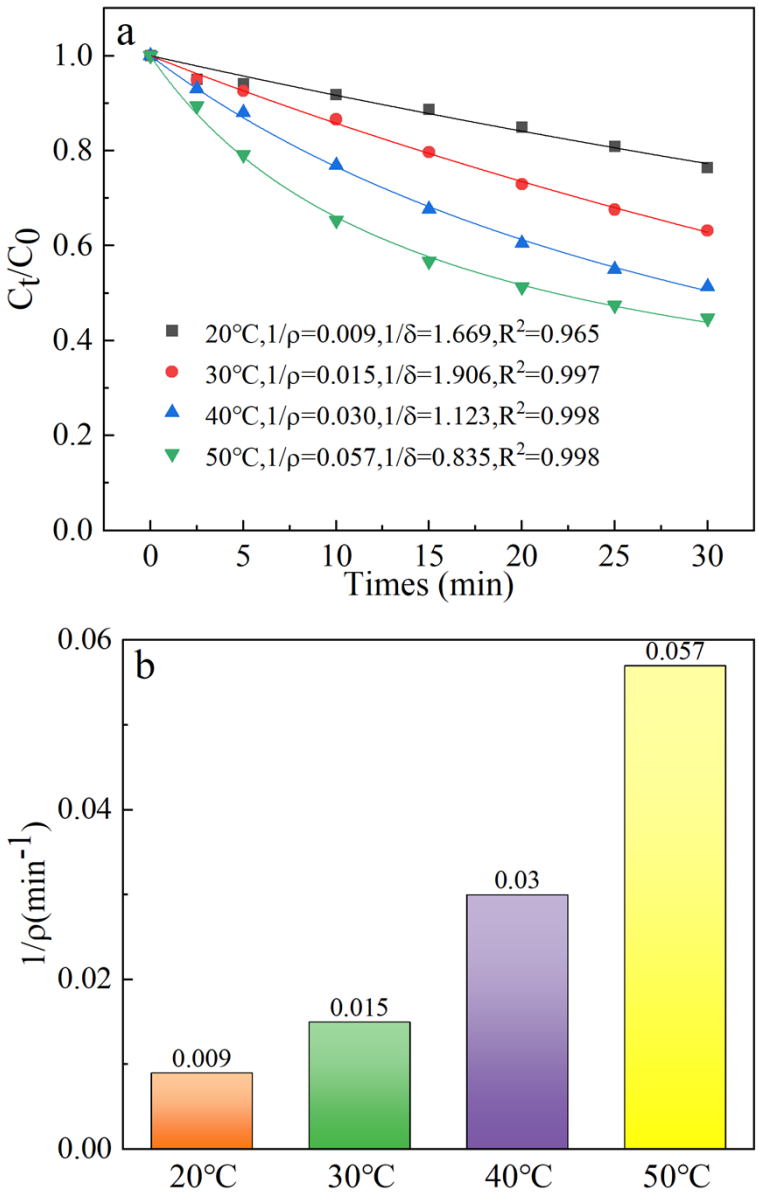

Fig.S7 Fitting curves of TC degradation by PMS self under different temperature (a), and the corresponding initial degradation rates (b).

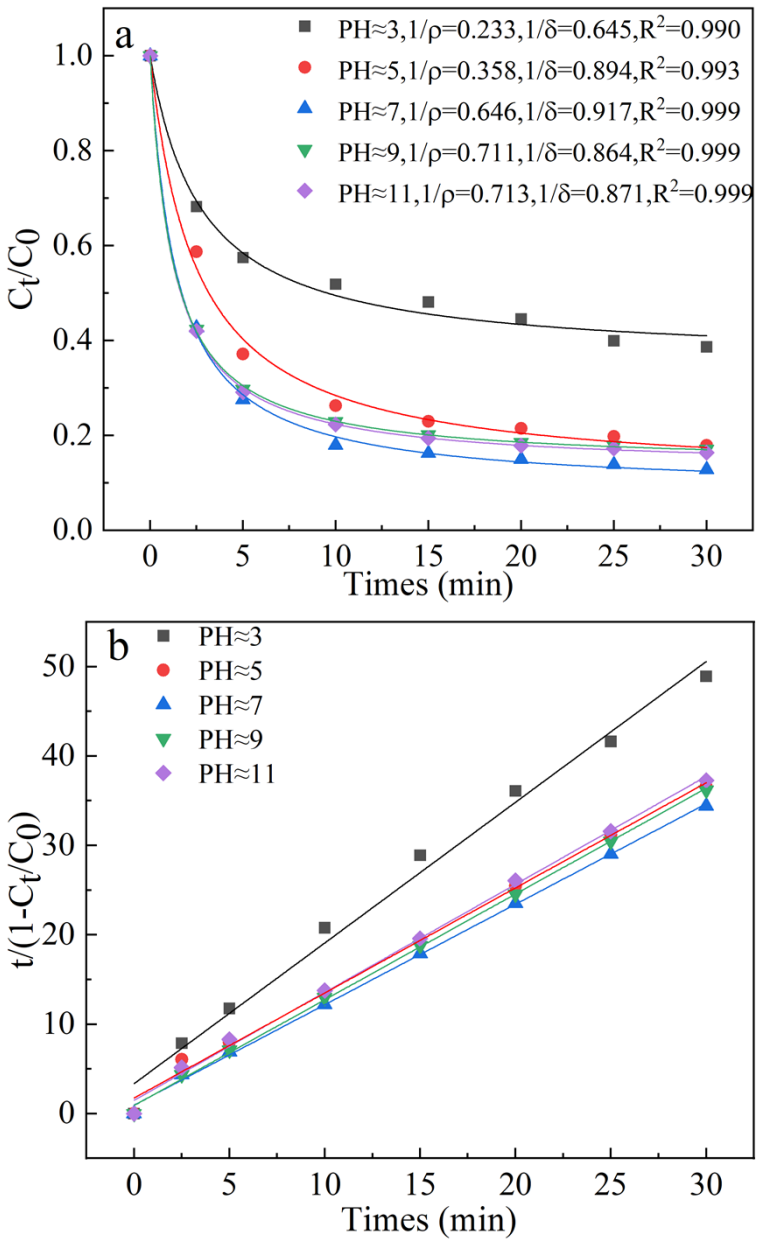

Fig.S8 Fitting curves of TC degradation by CuO/MCSA-1 under different pH values (a), and the corresponding kinetic models (b).

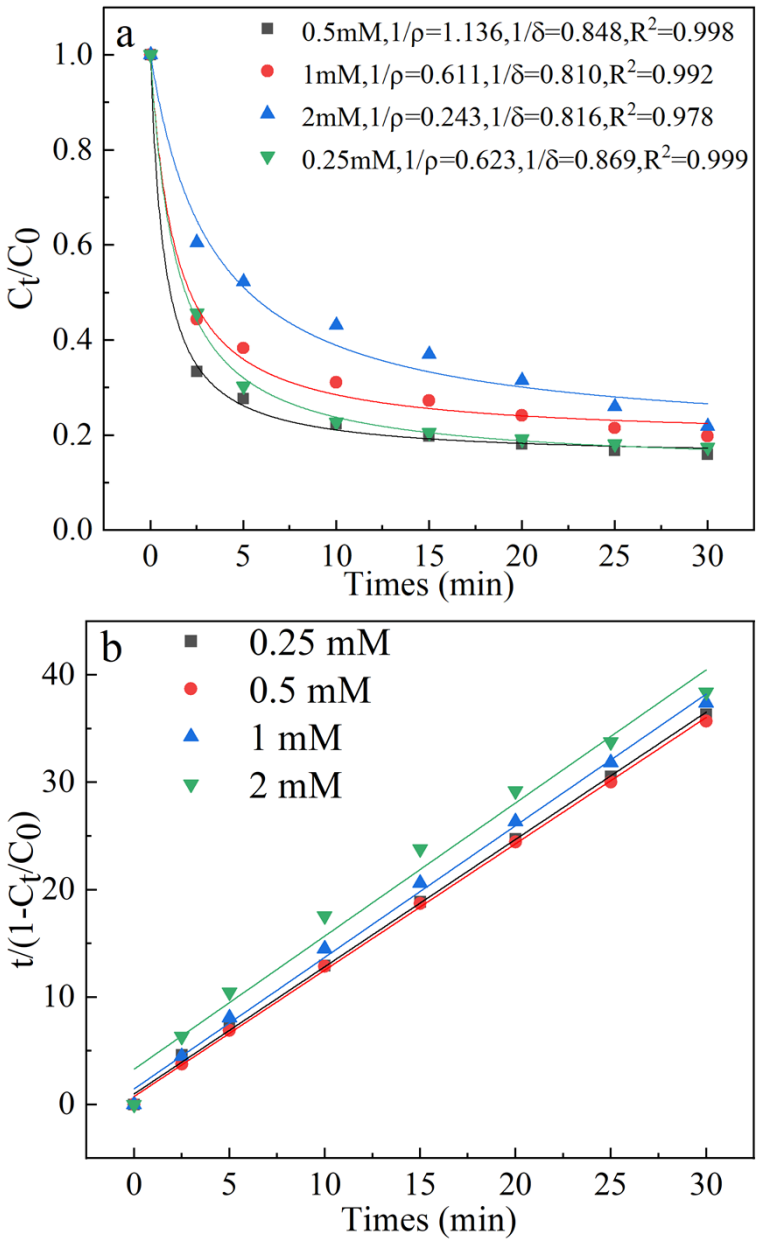

Fig.S9 Fitting curves of TC degradation by CuO/MCSA-1 with different PMS concentration (a), and the corresponding kinetic models (b).

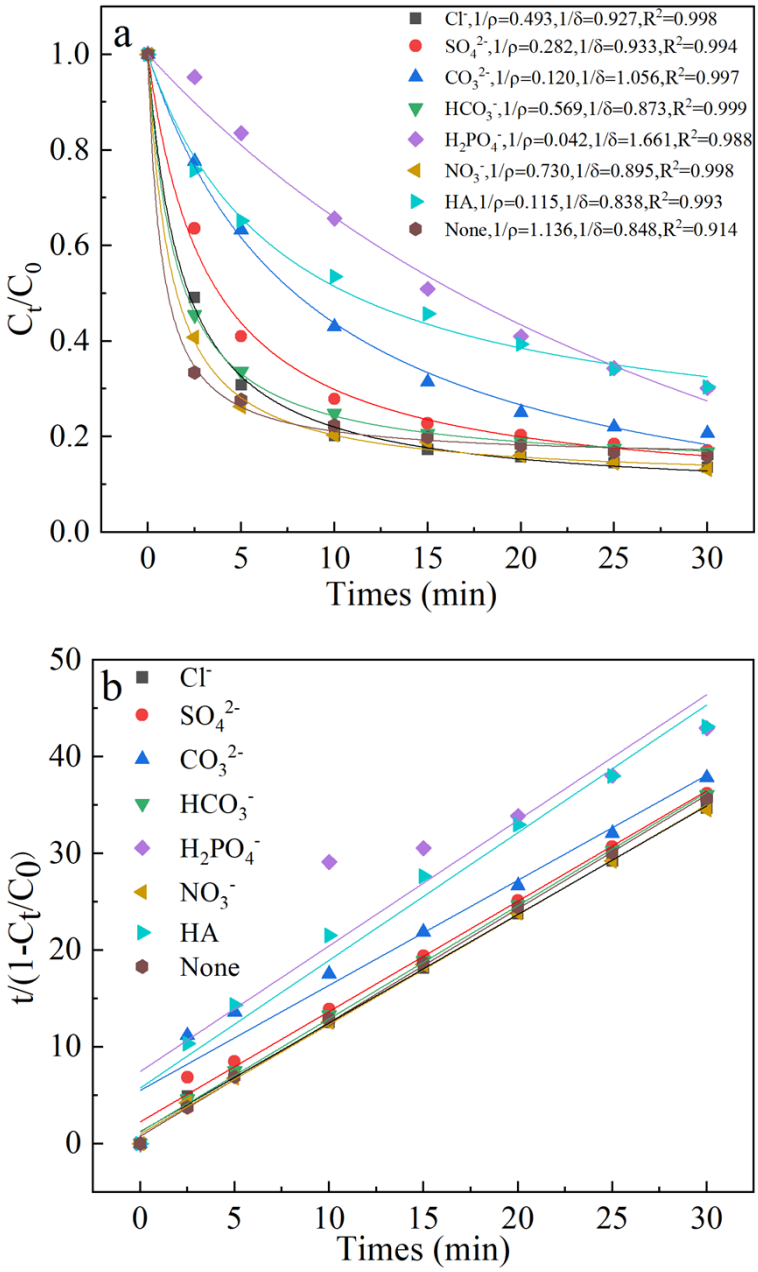

Fig.S10 Fitting curves of TC degradation by CuO/MCSA-1 after adding 2mM anion or HA (a), and the corresponding kinetic models (b).

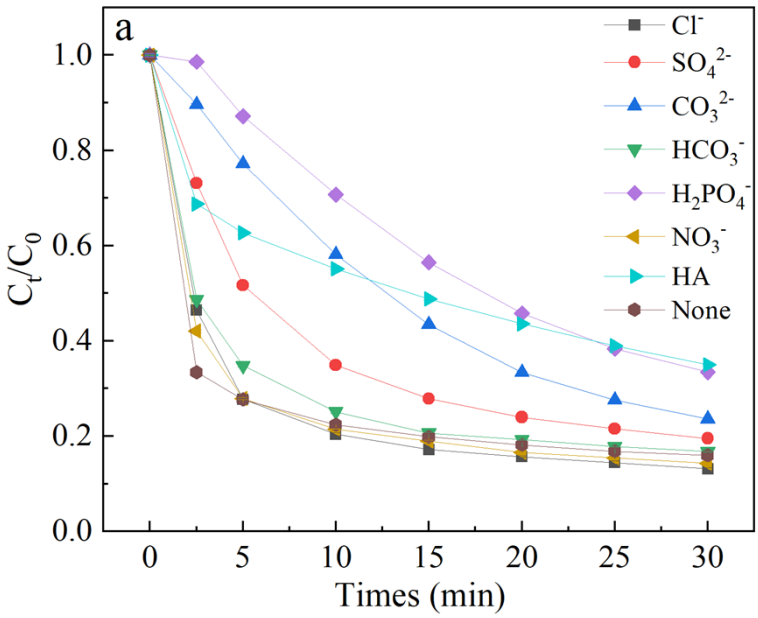
a
Cl-
SO4 2-
CO3 2-
HCO3-
H2PO4-
NO3-
HA
None
Ct/C0
Times (min)

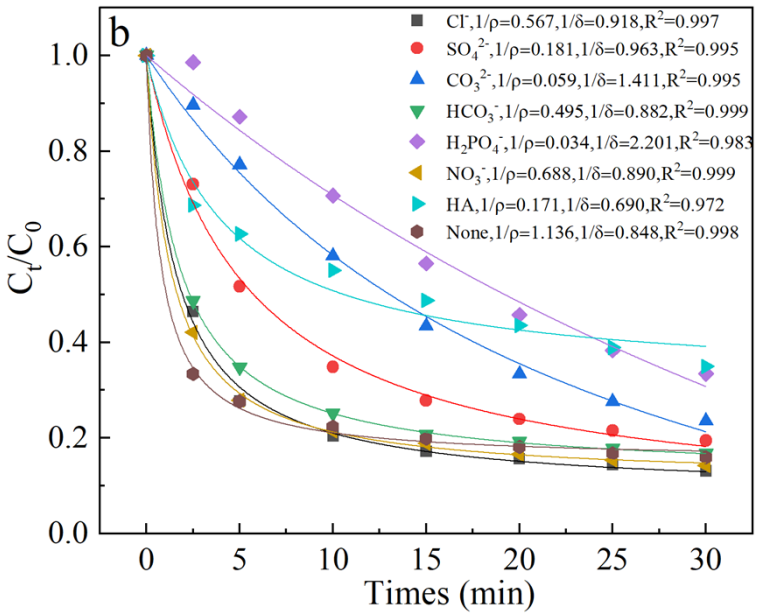
b
Cl-,1/ρ=0.567,1/δ=0.918,R2=0.997
SO4 2-,1/ρ=0.181,1/δ=0.963,R2=0.995
CO3 2-,1/ρ=0.059,1/δ=1.411,R2=0.995
HCO3-,1/ρ=0.495,1/δ=0.882,R2=0.999
H2PO4-,1/ρ=0.034,1/δ=2.201,R2=0.983
NO3-,1/ρ=0.688,1/δ=0.890,R2=0.999
HA,1/ρ=0.171,1/δ=0.690,R2=0.972
None,1/ρ=1.136,1/δ=0.848,R2=0.998
Ct/C0
Times (min)

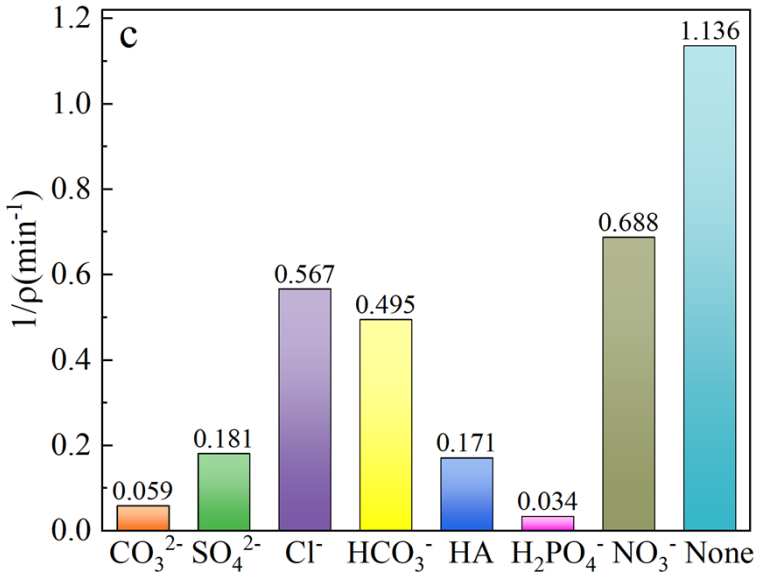
c
1/ρ(min-1)
0.059
0.181
0.567
0.495
0.171
0.034
0.688
1.136
CO3 2-
SO4 2-
Cl-
HCO3-
HA
H2PO4-
NO3-
None

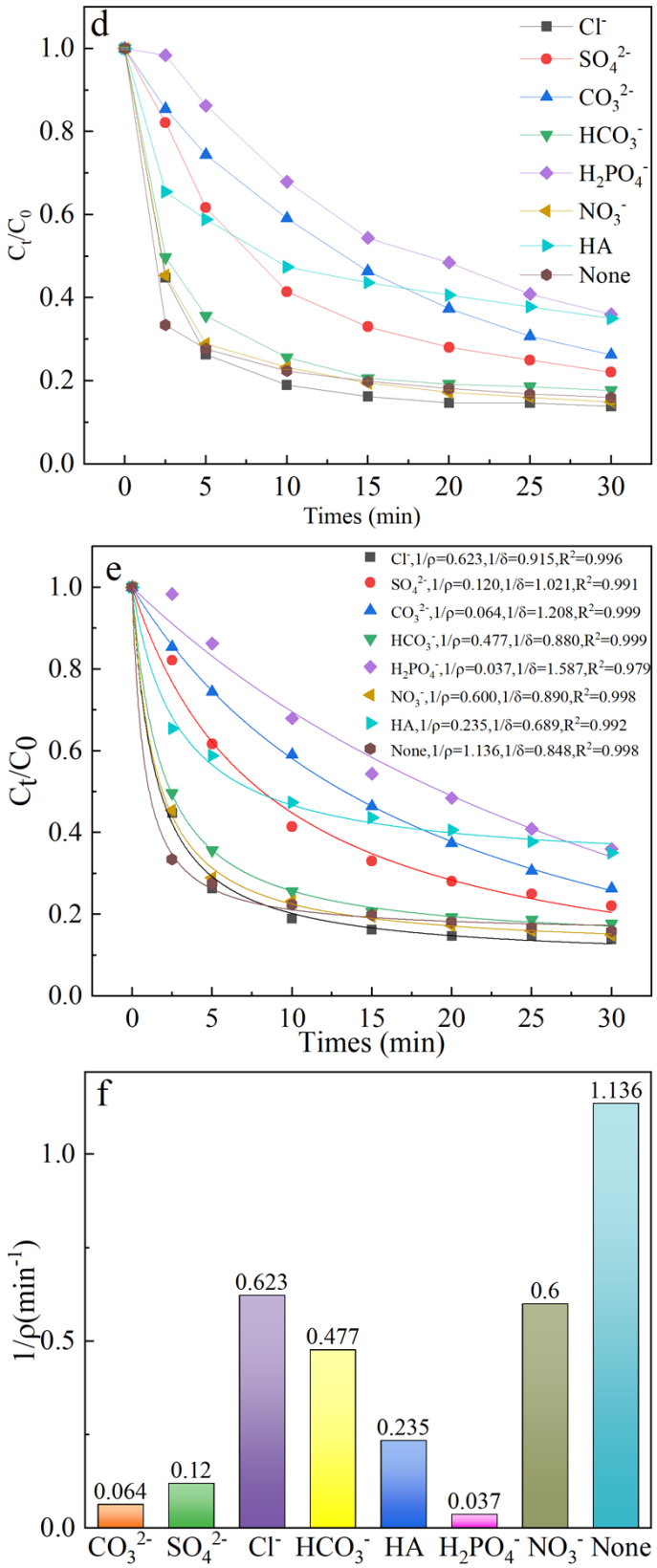

Fig.S11 TC degradation by CuO/MCSA-1 after adding 4 mM or 8 mM anion or HA (a, d),the corresponding fitting curves (b, e) and the corresponding initial degradation rate constants (c, f).

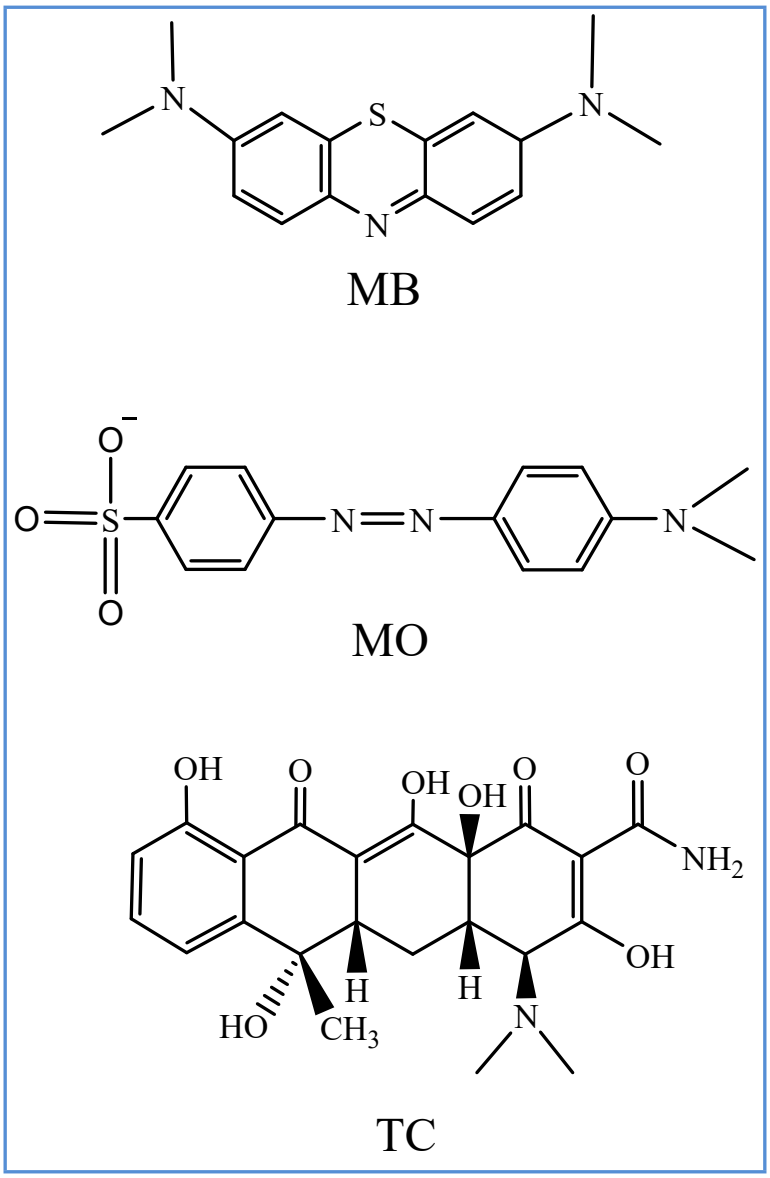

Fig.S12 the Structural formulas for corresponding organic pollutants

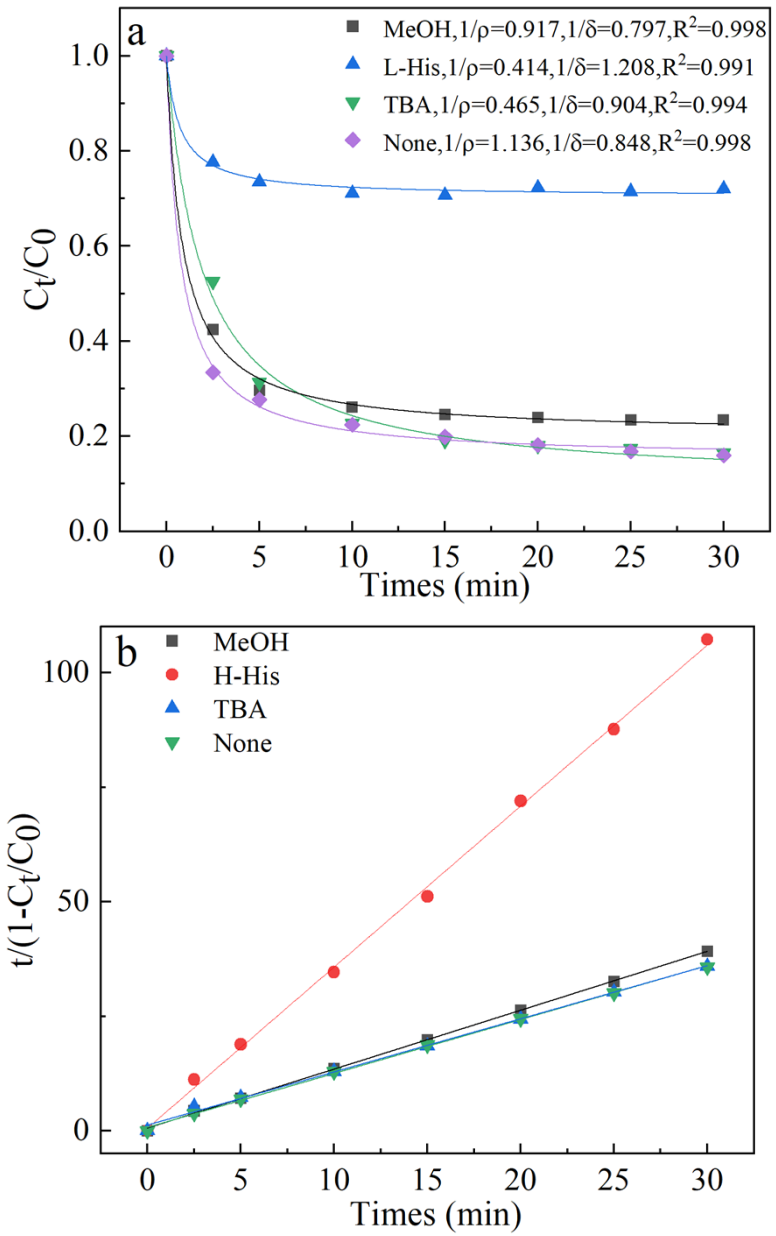

Fig.S13 Fitting curves of TC degradation by CuO/MCSA-1 after adding various scavengers (a), and the corresponding kinetic models (b).

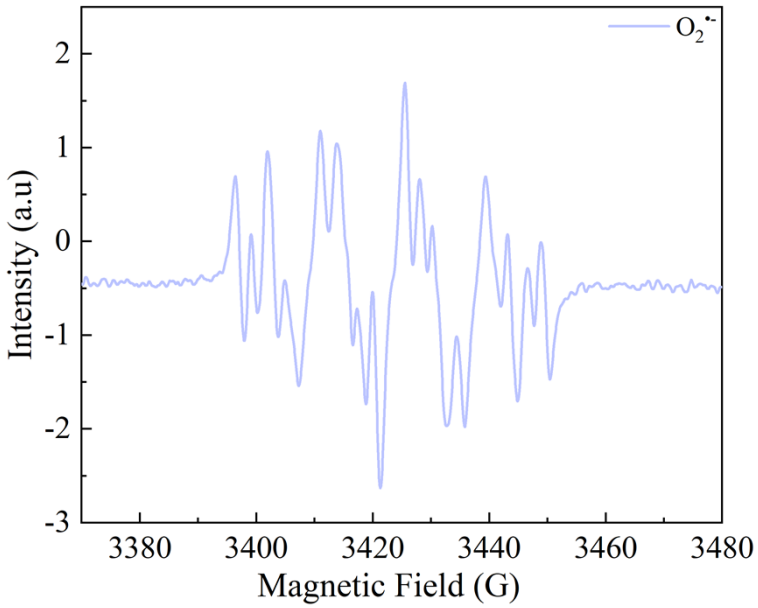

Fig.S14 EPR spectrum of $O_2^{\bullet-}$.

Fig.S15 Stability tests of CuO/MCSA over five consecutive cycles.